

1 RetroFun-RVS: a retrospective family-based
2 framework for rare variant analysis
3 incorporating functional annotations

4 Loïc Mangnier^{1,2,3}, Ingo Ruczinski⁴, Jasmin Ricard², Claudia Moreau⁵,
 Simon Girard⁵, Michel Maziade^{2,6}, Alexandre Bureau^{1,2,3*}

5 ¹ Department of Social and Preventive Medicine, Laval University,
6 Quebec City, QC, Canada

7 ² CERVO Brain Research Center, Quebec City, QC, Canada

8 ³ Big Data Research Center, Quebec City, QC, Canada

9 ⁴ Department of Biostatistics, Johns Hopkins Bloomberg School of
10 Public Health, Baltimore, MD, USA

11 ⁵ Department of Fundamental Sciences, University of Quebec in
12 Chicoutimi, Saguenay, QC, Canada.

13 ⁶ Department of Psychiatry and Neurosciences, Laval University,
14 Quebec City, QC, Canada. * corresponding author:
15 alexandre.bureau@fmed.ulaval.ca

16 **Funding**

17 Some data analyses were performed on computing resources from Compute
18 Canada. This work was partly funded by the Canadian Statistical Sciences
19 Institute through a Collaborative Research Team grant and by a National Sci-
20 ence and Engineering Research Council of Canada Discovery grant to A Bu-
21 reau. The Eastern Quebec Schizophrenia and Bipolar Disorder Kindred Study
22 was funded by a Canada Research Chair (#950-200810) in psychiatric genetics
23 of which Maziade is the Chair and by Canadian Institute of Health Research
24 grants (#MOP-74430, #MOP-114988, #PCG-155471 and #PJT-175122).

25 Abstract

26 A large proportion of genetic variations involved in complex diseases are rare
27 and located within non-coding regions, making the interpretation of underlying
28 biological mechanisms a daunting task. Although technical and methodological
29 progresses have been made to annotate the genome, current disease - rare-variant
30 association tests incorporating such annotations suffer from two major limita-
31 tions. Firstly, they are generally restricted to case-control designs of unrelated
32 individuals, which often require tens or hundreds of thousands of individuals to
33 achieve sufficient power. Secondly, they were not evaluated with region-based
34 annotations needed to interpret the causal regulatory mechanisms. In this work
35 we propose RetroFun-RVS, a new retrospective family-based score test, incor-
36 porating functional annotations. One of the critical features of the proposed
37 method is to aggregate genotypes while measuring rare variant sharing among
38 affected family members to compute the test statistic. Through extensive sim-
39 ulations, we have demonstrated that RetroFun-RVS integrating networks based
40 on 3D genome contacts as functional annotations reaches greater power over the
41 region-wide test, other strategies to include sub-regions and competing methods.
42 Also, the proposed framework shows robustness to non-informative annotations,
43 keeping a stable power when causal variants are spread across regions. We pro-
44 vide recommendations when dealing with different types of annotations or family
45 structures commonly encountered in practice. Application of RetroFun-RVS is
46 illustrated on whole genome sequence in the Eastern Quebec Schizophrenia and
47 Bipolar Disorder Kindred Study with networks constructed from 3D contacts
48 and epigenetic data on neurons. In summary we argue that RetroFun-RVS, by
49 allowing integration of functional annotations corresponding to regions or net-
50 works with transcriptional impacts, is a useful framework to highlight regulatory
51 mechanisms involved in complex diseases.

52 **Keywords:** Non-coding genome, Pedigree-based association tests, Variant
53 sharing, 3D genome

54 1 Introduction

55 Over the past few years with the democratization of whole-exome or whole-
56 genome sequencing data, important progresses have been made in the effort to
57 link genetic variations to phenotypes. Indeed, at population scale, Genome-
58 Wide Association Studies (GWAS) have provided useful resources to highlight
59 variants involved in diseases. However, these methods, in addition to requiring
60 tens or hundreds of thousands of individuals, are mainly restricted to common
61 variants, leaving an important part of heritability unexplained¹. In fact, stud-
62 ies have shown that the individual genetic risk is also substantially influenced
63 by rare variants (minor allele frequency (MAF) $\leq 1\%$),^{2,3}. In addition to be-
64 ing rare, variants influencing disease risk tend to be located within non-coding
65 regions, making the underlying biological mechanisms difficult to interpret⁴.
66 Thus, the tremendous amount of rare variants located within non-coding re-
67 gions brings new challenges to identify new causal variants involved in diseases,
68 and accounting for their functional impacts remains crucial from a fine-mapping
69 perspective, hence translational medicine applications⁵.

70 Methods have been proposed to overcome the challenge of sparsity. Indeed,
71 because variants are rare, methods testing them in an unitary fashion perform
72 badly⁶. Thus, rare-variants association tests (RVATs) are methods aggregating
73 genotypes across several variant sites within a gene, pathway or regions func-
74 tionally close. By collapsing variants over regions, these methods considerably
75 reduce the number of tests throughout the genome, hence increasing statistical
76 power. Among them, burden tests were initially proposed and are powerful
77 when all variants across regions show a homogeneous effect^{7,6}. However, when
78 regions combine both deleterious and protective variants, burden tests compar-
79 ing cases to controls suffer from a substantial decrease of power. Alternatives
80 to address this limitation have been proposed^{8,9}. One of the critical features
81 of RVATs is that they can be expressed through regression models, allowing
82 either the integration of covariates or variant weights, either fixed (based on the
83 MAF), or estimated in a data adaptive manner^{6,10}.

84 An alternative approach is to exploit family-based studies. In addition to
85 reducing genetic heterogeneity, pedigree-based studies have been shown to have
86 more power than population-based approaches for detecting rare variants, when
87 an enrichment of risk variants among families is expected^{11,12,13}. Information
88 provided by variants segregating with the disease, even imperfect, can be ex-
89 ploited to highlight new causal variants, giving a second breath to studies in ex-
90 tended pedigrees¹⁴. Recent methods based on identity-by-descent (IBD) or com-
91 bining both linkage approaches and RVATs have been developed^{15,16,17}. These
92 approaches focus on, or can be restricted to only affected family members, when
93 these are expected to contribute more information than unaffected subjects¹⁸.
94 Affected-only designs have a long tradition in gene-gene or gene-environment
95 interaction analysis and have been extended to family-based studies, requir-
96 ing smaller sample sizes to reach equivalent power, compared to considering
97 unrelated case-only individuals, which is an appealing feature in practice¹⁹.
98 However, in many cases, knowing and defining the sampling scheme is difficult,

99 hence impossible, pushing researchers to consider retrospective approaches. Ret-
100 rospective models by conditioning on phenotypes do not explicitly model the
101 ascertainment process. Successful applications of such methods have been shown
102 for common¹⁸ and rare variants²⁰.

103 A limitation of all the above methods is that none of them currently inte-
104 grates external information on biological mechanisms involved in diseases. How
105 to leverage information on non-coding regulatory elements in the detection of
106 variants influencing disease risk remains an open question. Thus, there is an in-
107 creasing interest in using external information for this task, and hence highlight-
108 ing the biological mechanisms. Recent methods, such as FST²¹ or FunSPU²²
109 have proposed to adaptively test functional annotations under a general RVAT
110 framework. These methods have shown substantial increases in power when at
111 least one functional score is predictive for the effect of variants on the trait,
112 while they show robustness when no annotations were predictive for variant
113 impact on the trait, revealing new causal variants involved in complex traits.
114 Moreover, the multiple ways to define test statistics corresponding to several
115 functional annotations created a need for combining p-values within a given re-
116 gion to assess the association with a trait, while adjusting for multiplicity. Liu
117 et al.²³ have proposed the aggregated Cauchy association test (ACAT), a pow-
118 erful statistical framework combining p-values in an efficient way, not requiring
119 resampling procedures, nor independent p-values nor explicit models for corre-
120 lations. This facilitating applications even at the genome-wide scale. Although
121 these set-based tests have made possible the discovery of new regions involved
122 in complex diseases, they required very large sample sizes of unrelated subjects.

123 More recently, with the striking development of methods detecting regula-
124 tory elements such as enhancers^{24,25}, progresses have been made in associating
125 non-coding SNPs to their target genes^{26,27}. Subsequently, some authors have
126 proposed to incorporate this information within statistical frameworks. Ma
127 et al.²⁸ have demonstrated that long range 3D interactions between genes and
128 enhancers add information for the integration of non-coding regulatory regions
129 within gene-based frameworks. This model, consistent with previous studies,
130 only considers pairs of gene-enhancer²⁹. Frameworks extending gene-enhancer
131 pairs to Cis-Regulatory Hubs (CRHs), networks encompassing up to several
132 genes and active enhancers have been proposed³⁰. CRHs have been shown
133 to be a relevant model in schizophrenia etiology, explaining more heritability
134 than tissue- and non-tissue- specific elements, and being more effective to link
135 noncoding SNPs to differentially expressed genes in schizophrenia compared to
136 Topologically Associated Domains (TADs) or pairs of gene-enhancer. To our
137 knowledge, no study to date has proposed to integrate functional annotations
138 within a family-based RVAT framework, while allowing the incorporation of
139 discontinuous genomic regions involved in 3D-based networks.

140 In this paper, we propose RetroFun-RVS (Retrospective Functional Rare
141 Variant Sharing), a model, allowing the integration of functional annotations
142 under a family-based design considering only affected individuals. Through ex-
143 tensive simulation studies, we have demonstrated that RetroFun-RVS integrat-
144 ing CRHs as functional annotations is a more powerful approach to detect causal

145 variants over other strategies, while well controlling the Type I error rate. We
146 provide recommendations when dealing with different types of functional scores
147 or pedigree structures. Finally, illustrating RetroFun-RVS on the whole genome
148 sequence in the Eastern Quebec Schizophrenia and Bipolar disorder Kindred
149 study we have demonstrated that integrating 3D-based functional annotations
150 through networks is a relevant strategy to gain power for detection of causal
151 variants, while highlighting the underlying biological mechanisms involved in
152 diseases.

153 2 Material and Methods

154 2.1 Notations and Model

155 Suppose that we have N subjects within F families, where n_f is the number of
156 individuals for the f^{th} family. Let's define Y , a binary vector of phenotypes, G
157 a $N \times p$ matrix of genotypes for rare variants, coded as unordered, discrete vari-
158 ables. Assuming a log-additive model for the individual SNP effect on disease
159 risk, under the assumptions of rare disease for all genotypes (i.e. weak vari-
160 ant penetrance) and of conditional independence of the phenotypes of different
161 individuals given their genotypes and considering only affected individuals, fol-
162 lowing Schaid et al.¹⁸, the retrospective likelihood for one family can be written
163 as:

$$P(G|Y) = \frac{\exp(\sum_{i \in D} \sum_{j=1}^p \beta_j x_{ij}) P(G)}{\sum_{G^*} \exp(\sum_{i \in D} \sum_{j=1}^p \beta_j x_{ij}^*) P(G^*)}$$

164 where D is the subset of affected members in the family, while x_{ij} is a con-
165 densed notation for $x(G_{ij})$, the number of minor alleles $\{0, 1, 2\}$ for variant j in
166 individual i in the multilocus genotype configuration G for all family members.
167 Also, we assume that only one copy of the minor allele was introduced once by
168 a family founder, implying x_{ij} can only take the values 0 or 1 in the absence
169 of inbreeding in the family (occasional genotypes with 2 variant alleles may be
170 recoded as $x_{ij} = 1$ with little impact on the results). In presence of inbreeding
171 and/or cryptic relatedness among family founders, homozygous genotypes for
172 rare alleles are expected and are allowed in the RetroFun-RVS implementation
173 using options described in the Supplementary Material and Methods.

174 In Schaid et al.¹⁸, $P(G)$ is the unconditional genotype probability and de-
175 pends on MAF, which needs to be estimated in practice. However, obtaining
176 accurate estimates of rare variant MAFs in a population is difficult. Instead, we
177 opted for conditioning the probability on the event of observing at least one a
178 copy of each RV j present in the family (i.e., $\sum_i x_{ij} \geq 1$) as in¹⁵. In addition,
179 we combined this conditional probability with the assumption that the variant
180 frequency tends to 0, hence the probability does not depend on MAF and there-
181 fore the computation does not require external variant frequency estimates. In
182 this context, the genotypes can be interpreted as rare variant sharing patterns
183 (referring to as RVS in the method name). The sum in the denominator is over
184 all genotype configurations respecting the condition within the given pedigree,

185 where G^* denotes one particular configuration. Since we expect that risk vari-
 186 ant effects dominate protective variant effects in the score test statistic when
 187 considering only affected individuals (Supplementary Materials and Methods
 188 and Figure S1), we propose to adapt the retrospective framework for a burden
 189 test^{7,6}. Hence, we can express β_j the effect of the j^{th} variant through $w_j\beta_0$
 190 where w_j is usually a weighting function to specify variant effects through a
 191 function of MAF.

192 As suggested by He et al.²¹, the effect for the j^{th} variant can be partitioned
 193 into effect parameters γ_k with respect to functional annotations $Z_{jk}, k = 1 \dots q$.
 194 Consequently, under a burden test framework this leads to:

$$\beta_j = w_j \sum_{k=0}^q Z_{jk} \gamma_k$$

195 with $Z_{j0} = 1$ and γ_0 corresponding to the original burden test parameter.
 196 Intuitively, this partition of the variant effect allows a modulation of the variant
 197 effect based on MAF and functional annotations. Moreover, when no predictive
 198 functional annotations are present for the trait, the burden of all p variants
 199 may nonetheless capture an overall effect on risk, and testing γ_0 ensures the
 200 combined test has some power. When at least one annotation is predictive, the
 201 partitioned model offers increased power over the original test²¹.

202 Now combining the retrospective likelihood model described by¹⁸ and the
 203 decomposed variant effect, we obtain:

$$P(G|Y) = \frac{\exp(\sum_{i \in D} \sum_{j=1}^p w_j x_{ij} \sum_{k=0}^q Z_{jk} \gamma_k) P(G)}{\sum_{G^*} \exp(\sum_{i \in D} \sum_{j=1}^p w_j x_{ij}^* \sum_{k=0}^q Z_{jk} \gamma_k) P(G^*)}$$

204 Thus for the k^{th} functional annotation the score function S_k summed across
 205 the F families is :

$$S_k(\gamma) = \sum_{f=1}^F \left(\sum_{j=1}^p w_j Z_{jk} \left(\sum_{i \in D} x_{fij} - \frac{\sum_{G_f^*} \sum_{i \in D} x_{fij}^* \exp(\sum_{j=1}^p w_j \sum_{k^*=0}^q Z_{jk^*} \gamma_{k^*} \sum_{i \in D} x_{fij}^*) P(G_f^*)}{\sum_{G_f^*} \exp(\sum_{j=1}^p w_j \sum_{k^*=0}^q Z_{jk^*} \gamma_{k^*} \sum_{i \in D} x_{fij}^*) P(G_f^*)} \right) \right)$$

206 Intuitively, this quantity can be seen as the difference between the observed
 207 genotype value and the expected value, weighted by MAF and functional an-
 208 notations. Setting γ to 0, we obtain the score statistic for the k^{th} functional
 209 annotation:

$$S_k(0) = \sum_{f=1}^F \left(\sum_{j=1}^p w_j Z_{jk} \left(\sum_{i \in D} x_{fij} - \sum_{G_{fj}^*} \sum_{i \in D} x_{ij}^* P(G_{fj}^*) \right) \right)$$

210 The genotype probability required $P(G_{fj})$ is for a single variant configura-
 211 tion in family f and can be computed using RVS³¹. Q_k is the test statistic cor-
 212 responding to $S_k(0)$, asymptotically following a normal distribution with mean
 213 0 and variance obtained by combining sharing pattern probabilities under the

214 null and observed genotypes within families. Moreover, simplifications may be
215 obtained from assumptions on the linkage disequilibrium structure (See Supple-
216 mentary Materials and Methods). However, we observed when only few variants
217 are expected within a functional annotation or a small number of families is ob-
218 served that resampling procedures may be required to adequately control the
219 Type I error rate (See next sub-section Bootstrap procedure using rare variant
220 sharing patterns).

221 For testing multiple functional scores within a single unified test $H_0 : \forall k, \gamma_k =$
222 0 vs $H_1 : \exists k, \gamma_k > 0$, we then propose to combine $q + 1$ single p-values corre-
223 sponding to the q functional annotations and the original burden with ACAT²³.
224 Briefly, ACAT aggregates individual p-values and approximates the test statis-
225 tic (and the subsequent p-value) based on a Cauchy distribution. So, for $q + 1$
226 tests in a region of interest, the ACAT statistic can be written as:

$$T_{ACAT} = \sum_{k=0}^q \tan((0.5 - p_k)\pi)$$

227 which follows approximately a Cauchy distribution under H_0 .

228 2.2 Bootstrap procedure using rare variant sharing pat- 229 terns

230 We propose a weighted non-parametric bootstrap procedure in order to compute
231 empirical p-values. Basically, genotypes were generated conditionally on the
232 number of observed variants in a family, considering the rare variant sharing
233 patterns occurring among family members. This procedure only requires the
234 aggregated genotypes across affected individuals e.g., $X_{fj} = \sum_{i \in D} x_{fij}$ and the
235 sharing pattern probabilities for a given family f , e.g., $P(G_{fj})$. We apply the
236 following procedure for estimating the null distribution of the test statistic:

- 237 • Sample aggregated genotypes for the p_f variants in family f across the F
238 families $\{\tilde{X}_{11}^b, \dots, \tilde{X}_{1p_1}^b, \dots, \tilde{X}_{F1}^b, \dots, \tilde{X}_{Fp_F}^b\}_{1 \leq b \leq B}$ using the sharing pat-
239 tern probabilities $P(G_{fj})$ obtained with RVS³¹.
- 240 • Construct the test statistic \tilde{Q}_k^b .
- 241 • Compute empirical p-values for all k , $p\text{-value}_k = \frac{1}{B} \sum_{b=1}^B I(\tilde{Q}_k^b \geq Q_k)$.
- 242 • ACAT-combined p-values are then obtained using empirical p-values in-
243 stead of asymptotic p-values over the $q + 1$ functional annotations.

244 Because the B bootstrap samples require only one set of rare variant sharing
245 probabilities for all families, they only need to be computed once, hence increas-
246 ing the computational performance, ensuring accurate estimation of p-values.

247 3 Numerical Simulations

248 We adopted the principle that CRHs are the annotations capturing best the
249 causal variants, with simpler annotations capturing causal variants to a lesser
250 extent. We thus selected a TAD in iPSC-derived neurons encompassing four
251 CRHs showing different complexities (two genes-five enhancers (CRH1); two
252 genes-two enhancers (CRH2); one gene-one enhancer (CRH3); one gene-four
253 enhancers (CRH4)) to setup the simulation study. See Table S1 and³⁰ for
254 more details. Genotypes were simulated based on observed variant sites and
255 their corresponding MAF for the European population from the 1000 Genome
256 Project database (phase 3). We extracted the 510 rare ($MAF \leq 1\%$) coding non-
257 synonymous and within-enhancer non-coding single nucleotide variants from
258 the TAD 800 kb (chr1:24100000-24970000). Using RarePedsim³², we generated
259 sequence data over the above 800 kb region for 270 affected subjects in the
260 primary sample of 52 pedigrees ranging from small to extended (Figures 1 and
261 S2) Families were simplified by removing inbreeding loops. For both Type I
262 error rate and power evaluation, the dichotomous phenotype was assumed to
263 follow a logistic model without covariates and with a population prevalence of
264 1%. Details on pedigree structures under the different scenarios were provided in
265 Table S2. We focused on evaluating the ACAT-combined p-values. Importantly,
266 to avoid large departures from the asymptotic distribution of RetroFun-RVS,
267 we only considered functional annotations with a number of families greater
268 than five. We also explored additional scenarios considering pedigrees of small
269 to moderate size, families with a varying number of affected members and with
270 presence of inbreeding. Details and results for these setups were provided in the
271 Supplementary Numerical Simulations.

272 3.1 Type I Error Simulations

273 To determine whether the proposed framework preserves the desired Type I er-
274 ror rate, genotype data were generated unconditional on the affection status for
275 family members. We specified a null effect for variants observed in families, i.e.,
276 odds-ratio (OR) = 1. Generating ten thousand replicates, we first examined the
277 performance of RetroFun-RVS_{CRHs}, which is RetroFun-RVS applied to CRHs
278 and including variants over the entire TAD as global burden, with alternative
279 definitions of regions to be included as functional scores: RetroFun-RVS_{Pairs},
280 RetroFun-RVS_{Genes}, and RetroFun-RVS_{Sliding-Window}, for the method consid-
281 ering pairs of gene-enhancers, genes and a 10 Kb sliding window, respectively
282 (Figure 2).

283 3.2 Empirical Power Simulations

284 We set 2% of the variants over the entire region to be risk variants as suggested
285 before²⁸, also performing simulations with 1% of risk variants as a sensitiv-
286 ity analysis. Genotypes were generated conditional on the affection status for
287 each pedigree member assuming a multiplicative model with fixed variant ef-

288 fect, i.e., not depending on the MAF. Simulating one thousand replicates, we
289 considered different scenarios where we varied the proportion of causal variants
290 found in CRHs: 100%, 75% and 50% of causal variants (OR=5) were located
291 within one CRH. The remaining variants being neutral (OR=1). This sce-
292 nario is expected when variants are concentrated within elements functionally
293 close. These three proportions correspond to the most advantageous scenario
294 where all causal variants are within the same region and two mixed scenar-
295 ios where signal is spread across the sequence of the region at different de-
296 grees. Our first evaluation assessed the gain of power by incorporating CRHs
297 as functional annotations over the test including no scores (referred to as Bur-
298 den Original). We also compared RetroFun-RVS_{CRHs} with others strategies to
299 incorporate regions as functional annotations: RetroFun-RVS_{Pairs}, RetroFun-
300 RVS_{Genes}, and RetroFun-RVS_{Sliding-Window}, for the method considering pairs
301 of gene-enhancers, genes and a 10 Kb sliding window, respectively (Figure 2).
302 Also, we assessed the performance in terms of power of our method compared
303 to existing approaches namely, RVS¹⁵ and RV-NPL¹⁷ (Figure S3). Power was
304 evaluated as the proportion of p-values less than $\alpha = 8.33 \times 10^{-6}$, correspond-
305 ing to the Bonferroni-adjusted 0.05 significance level when testing six thousand
306 independent regions across the genome, corresponding to three thousand TADs
307 (the average number of TADs found in our previous study across cell-types or
308 tissues³⁰, while permitting the same number of additional domains of interest,
309 i.e., outside TADs, to be tested. Results at lower proportion of risk variants
310 and considering small pedigrees are also reported.

311 4 Illustration on the Eastern Quebec Schizophrenia and Bipolar Disorder Kindred Study

312

313 To illustrate the application of RetroFun-RVS to a whole-genome sequencing
314 (WGS) study, we used data from the initial freeze of WGS on participants from
315 the Eastern Quebec schizophrenia and bipolar disorder kindred study. Signed
316 consent was obtained from all participants or from the parents for participants
317 under 18 years of age for collection of all data analyzed here, under the supervi-
318 sion of the University-affiliated neuroscience and mental health ethics commit-
319 tee.

320 A description of genomic sequencing and data quality control can be found
321 in the Supplementary Materials and Methods. For the present analysis we kept
322 the 28 families with at least two relatives affected by the broad definition of
323 schizophrenia, bipolar disorder and schizoaffective disorder in the Eastern Que-
324 bec Kindred Study³³. These 28 families included a total of 288 participants
325 with WGS, including 175 who were affected. Inbreeding loops where two par-
326 ents are first or second cousins were present in 6 families. All families of the
327 Eastern Quebec kindred study were connected in a single genealogy with a mean
328 completeness of 71% at the 10th generation back using the BALSAC database
329 (balsac.uqac.ca). Using that genealogy, we estimated to 0.0032 the mean kin-

330 ship between the founders of the 28 families included in this study (the subjects
331 who did not have parents in the 28 family structures before genealogy recon-
332 struction). We used that value to apply the correction for cryptic relatedness
333 to the RV sharing probabilities described by¹⁴ in the computation of the ex-
334 pected value, variance and covariance of the score statistics $S_k(0)$ under the
335 null hypothesis to obtain the asymptotic p-value of the tested variant sets. As a
336 sensitivity analysis, we also analyzed the data using the standard approach de-
337 scribed in subsection 2.1 in the simplified family structures without inbreeding
338 loops from the primary sample used for the simulation study, replacing ho-
339 mozygous rare genotypes by heterozygous ones. The bootstrap procedure was
340 applied to the variant sets yielding an asymptotic p-value below the significance
341 level Bonferroni-corrected for the number of tests performed.

342 Our study focused on rare autosomal SNVs and short indels. We defined
343 a rare variant as being absent or having a frequency < 0.01 in GnomAD non-
344 Finnish European sample and in a sample of 1,756 controls from the founder
345 Quebec population included in the CARTaGENE cohort (www.cartagene.qc.ca)³⁴.

346 We used as functional annotation the 1,633 CRHs defined by³⁰ in neurons
347 derived from induced pluripotent stem cells. We included the 1237 CRHs cov-
348 ering at least one retained rare SNV or short indel, and either comprised in a
349 single TAD (1042), overlapping two TADs (145) or outside any TAD (50). We
350 applied ACAT to combine p-values of the burden test and CRH-specific tests
351 in the 679 TADs with at least one rare SNV in a CRH entirely contained in the
352 TAD and tested the other CRHs individually, for a total of 874 tests.

353 5 Results

354 5.1 Simulation of Type I Error Rate

355 The results show that, when we considered CRHs as functional annotations
356 and accounted for variant dependence in the variance calculation, the Type I
357 error rate was well-controlled when combining p-values using ACAT (Figure
358 3). However, we observed slight false positive inflations when RetroFun-RVS
359 was applied with the independence variant structure or combining p-values us-
360 ing Fisher’s combined probability method (Figure S4A-S4B). Moreover, results
361 for RetroFun-RVS_{CRHs} with no functional annotations and for each individual
362 score show that the approach with covariance terms is either well calibrated
363 or slightly conservative (Figure S4D to S4F). In addition, the method shows
364 moderate Type I error rate inflation when applied to small to moderate family
365 structures, increasing when assuming variant independence (Figure S5). Fur-
366 ther investigations have shown that Type I error depends on the structure con-
367 sidered (Figure S6). When investigating scenarios in presence of inbreeding,
368 we observed that RetroFun-RVS_{CRHs} considering homozygous configurations
369 slightly reduces Type I error inflation in presence of a modest number of inbred
370 families, compared to results where consanguinity is left untreated (Figure S7A),
371 consistent with the improvement in Type I error control achieved by the depen-

372 dence correction. In contrast to our "only-inbred" scenario, where high level of
373 false positives are observed even when considering homozygous configurations
374 (Figure S7B).

375 Turning now to pairs and genes as functional annotations, we observed mod-
376 erate inflation of the Type I error rate in extended pedigrees, even when con-
377 sidering variant dependence, while for 10Kb sliding windows the Type I error
378 rate inflation was more severe (Figure S8). We attempted to discard 10 kb win-
379 dows with few variants, and observed that Type I error control was achieved
380 on windows encompassing 30 variants or more but few windows met this re-
381 quirement (results not shown). Moreover, the bootstrap procedure applied to
382 RetroFun-RVS_{Pairs}, RetroFun-RVS_{Genes} and , RetroFun-RVS_{Sliding-Window} to
383 compute p-values empirically provides Type I error rate control, although being
384 conservative, particularly for functional annotations encompassing few variants
385 (Figure S9). To summarize, the results show that RetroFun-RVS with asymp-
386 totic p-values is a valid approach when CRHs or a large region are considered in
387 extended pedigrees, despite being inflated to various degrees for others strate-
388 gies or certain family structures. Bootstrap p-values can be computed in these
389 instances to control the Type I error rate.

390 5.2 Power and Scalability Comparison Considering Differ- 391 ent Strategies to build Functional Annotations

392 In the first set of power evaluations, we assessed power under different scenar-
393 ios of causal variant distributions. Firstly, we compared RetroFun-RVS inte-
394 grating CRHs with the same method incorporating no functional annotation.
395 Consequently, when 100% and 75% of causal variants were within one CRH,
396 our method RetroFun-RVS_{CRHs} performed better than the original burden test
397 showing gains of 10% and 9%, while at 50% causal the power remains compa-
398 rable (Figure 4A). Also, considering only pedigrees of small to moderate size,
399 we observed that, even if both RetroFun-RVS_{CRHs} and the original burden test
400 without annotation exhibit lower power, the gain for RetroFun-RVS_{CRHs} be-
401 comes higher as the percentage of causal variant within the CRH of interest
402 increases (Figure S10). Congruent results were obtained when a lower propor-
403 tion of causal variants was considered, showing a minimal power gain of 10%
404 and a maximal increase of 125% (Figure S11). Therefore, our findings suggest
405 that substantial power gain can be achieved when CRHs are predictive for the
406 effect of variants on the trait, RetroFun-RVS_{CRHs} showing robustness when sig-
407 nal is spread across several CRHs. Then, we compared RetroFun-RVS_{CRHs} to
408 other strategies to integrate regions as functional annotations, namely RetroFun-
409 RVS_{Pairs}, and RetroFun-RVS_{genes}. Our results show that integrating CRHs as
410 functional annotations is a more powerful strategy compared to the other strate-
411 gies considered (Figure 4B). The power of RetroFun-RVS considering sliding
412 windows as functional annotations comparable to RetroFun-RVS_{CRHs} (Figure
413 S12) is likely explained by inflated Type I error rate. Globally our results fol-
414 low the same pattern when decreasing the proportion of causal variants (Figure
415 S13). In summary, RetroFun-RVS_{CRHs} exhibits power gains when CRHs show

416 high or modest percentages of causal variants. Also, the method is robust and
417 powerful under the different scenarios that we considered, that are, inclusion
418 of weakly predictive CRHs, small percentages of risk variants, and presence of
419 small families.

420 5.3 Power Comparison with Others Affected-Only Meth- 421 ods

422 In the second set of power evaluations, we compared RetroFun-RVS_{CRHs} with
423 other affected-only methods, namely RVS¹⁵ and RV-NPL¹⁷. Thus, to proceed
424 to fair comparisons between methods, we adapted RVS and RV-NPL to take
425 CRHs into account (See Supplementary Numerical Simulations). With 2% risk
426 variants, when we considered 75% of causal variants located within one CRHs,
427 we observed that RetroFun-RVS reaches greater power compared to compet-
428 ing methods (4C), exhibiting significantly shorter computing times (Table 1).
429 At lower proportions of risk variants, the new method remains more powerful
430 compared to RV-CHP or RVS, and equivalent to RV-NPL (Figure S14).

431 6 Illustration on the Eastern Quebec Schizophre- 432 nia and Bipolar Disorder Kindred Study

433 No ACAT-combined-over-TAD or single CRH p-value reached the significance
434 level $\alpha = 0.05/874 = 5.7 \times 10^{-5}$ corresponding to a Bonferroni correction
435 for the number of tests performed, after recomputing with the bootstrap the
436 asymptotic p-values below that level. As an illustration, we provide details
437 of the CRH with a bootstrap p-value = 0.00016 (asymptotic p = 0.000077)
438 to illustrate patterns of sharing that can be captured by RetroFun-RVS. The
439 original Burden p-value is 0.18, thus if variants in the CRH are true suscep-
440 tibility variants, this result would be aligned with our simulation studies in
441 which the unified test was more powerful with predictive functional annota-
442 tions. This CRH between positions 43998889 and 44492786 on chromosome 7
443 encompasses 11 genes (*PGAM2*, *POLM*, *AEBP1*, *DBNL*, *POLD2*, *RASA4CP*,
444 *YKT6*, *CAMK2B*, *SPDYE1*, *NUDCD3*, *POLR2J4*) and 19 enhancers. Import-
445 tantly, on the eight variants seen in at least one affected subject (in a total of
446 eleven families), four were located either in an intergenic or a genic enhancer,
447 impacting between one and ten genes simultaneously. These enhancers located
448 up to 343 Kb distance apart from their target genes (average 91Kb). This result
449 suggests that strategies linking non-coding variants to the nearest gene will fall
450 short in identifying the putative causal gene. We illustrated this result in Figure
451 S15. Figure S16 illustrates the family with the rare SNV shared by the most
452 affected subjects, including one who shares the rare allele with other affected
453 family members through unknown relations accounted for by the correction for
454 cryptic relatedness based on the kinship among founders.

455 7 Discussion

456 Most of rare genetic variations are located within non-coding regions, making
457 the underlying biological mechanisms through which they impact disease risk
458 difficult to interpret. Over the past few years, efforts were not only made in
459 annotating the genome but also integrating these annotations into statistical
460 frameworks^{21,22}. Although such methods have already been developed for un-
461 related subjects such as case-control samples, to our knowledge, no approach
462 to date has been proposed to integrate functional annotations within family-
463 based designs. In this paper we have presented RetroFun-RVS, a retrospective
464 burden test, integrating functional annotations considering only affected indi-
465 viduals within families. We have shown that binary annotations corresponding
466 to disjoint regions with regulatory impacts, such as CRHs, provide power gains
467 when such regions concentrate causal variants, outperforming other strategies
468 or competing methods (Figure 4), while well controlling the Type I error rate
469 in samples of families of various size and structure (Figure 3). Since regulatory
470 mechanisms are highly tissue- or context-dependent it can be challenging to
471 have the right tissue for the right trait, and misspecifying the model is likely
472 in practice. Thus, integrating the original burden test, corresponding to aggre-
473 gating all variants across a region, in RetroFun-RVS makes it robust, showing
474 stable power when functional annotations poorly predict the trait. Finally,
475 by computing p-values asymptotically, RetroFun-RVS is computationally faster
476 than competing methods, which often require permutation-based approaches or
477 exact probability computations to sharply control the Type I error rate.

478 The main rationale behind RetroFun-RVS is that risk variants are enriched
479 among affected individuals compared to the expected variant count based on
480 their relationships. Hence, one critical feature of our method is to aggregate
481 genotypes while measuring rare variant sharing among affected family members
482 to compute the test statistic. To implement an affected-only analysis, where
483 individuals are selected based on their disease status, we have adopted a ret-
484 rospective approach, considering genotypes as random, while conditioning on
485 phenotypes¹⁸. Also, since genotype probabilities do not depend on MAF under
486 the assumption that the variant frequency tends to 0, RetroFun-RVS necessi-
487 tates only familial information to compute these probabilities, in order to derive
488 the score statistic and its variance (See Material and Methods). This aspect is
489 central, since the variance terms need to be computed only once for the entire
490 set of families, which is computationally efficient even in presence of large pedi-
491 grees. Our rare variant assumption however implies that genotypes homozygous
492 for the rare allele are impossible in the absence of inbreeding. Data simulated
493 for Type I error and power assessments did contain the small number of ho-
494 mozygous rare genotypes expected for variants with $MAF = 1\%$. Conversion to
495 heterozygous genotypes did not increase Type I error rate compared to removing
496 the variants with homozygous rare genotypes, so we only showed results with
497 the conversion to heterozygous genotypes. Also, we observed that RetroFun-
498 RVS controls the Type I error rate well in the presence of a small to modest
499 number of inbred families (Figure S7A). Thus, if in practice cryptic relatedness

500 or inbreeding are expected for only a small proportion of families, we suggest to
501 use RetroFun-RVS without considering homozygous configurations. Indeed, de-
502 pending on the inbreeding configuration, computational times may be extremely
503 long, limiting applications for large families. Moreover, our simulation studies
504 have demonstrated that in the presence of a high proportion of inbred families
505 or a high level of inbreeding, RetroFun-RVS may suffer from severe inflation
506 without allowing homozygous configurations, and some inflation remains even
507 when handling homozygosity (Figure S7B). In an intermediate scenario such as
508 the application to the Eastern Quebec Kindred Study with widespread cryptic
509 relatedness and some inbreeding, considering homozygous configurations may
510 provide a gain in power and is recommended.

511 In addition to being computationally effective, RetroFun-RVS is more power-
512 ful than other affected-only competing methods, under certain scenarios (Figure
513 4C, Figure S13). For example, compared to RVS, on which RetroFun-RVS is
514 built upon, but which can only analyze between one and five rare variants si-
515 multaneously in the pedigree sample used in the simulation study, we reached
516 greater power by testing tens of variants together in annotated regions, or even
517 hundreds of variants in the absence of annotations. It is noteworthy that the
518 simulated variant ORs did not depend on the variant MAF due to limitations
519 of the simulation software. The MAF-dependent variant weighting scheme of
520 RetroFun-RVS was thus misspecified in the power evaluation. Greater power
521 gains of RetroFun-RVS over the competing methods ignoring variant MAF could
522 have been achieved had the variant ORs be inversely related to MAF.

523 Although the score test was well-calibrated and powerful in our primary
524 sample covering a large size range from small families to extended pedigrees, we
525 have detected modest Type I error rate inflation with another sample of small to
526 moderate family structures (Figure S5). Additional investigations have shown
527 that RetroFun-RVS controls the false positive rate accurately under certain fam-
528 ily structures, while providing slightly conservative or inflated quantile-quantile
529 plots for other structures (Figure S6). Since we did not observe clear associations
530 between the number of affected individuals and false positive rates, we argue
531 that the inflation observed is more a question of family structure than family
532 size. We argue that RetroFun-RVS controls the Type I error rate adequately
533 with typical family samples consisting in combinations of small to extended
534 pedigrees. On a related note, some analyses have shown that Type I error rate
535 or power are highly dependent on the number of variants present in the region
536 of interest. Indeed, we have observed that when large numbers of variants are
537 considered, RetroFun-RVS might provide conservative results involving some
538 power loss (Figure S4C), while a small number of variants tends to offer in-
539 flated Type I error rate (Figure S8). Complementary analyses are needed to
540 inspect the empirical relationship between size of region and performance. We
541 recommend in practice to use the dependence-adjusted model. Bootstrap pro-
542 cedures (Figure S9) might be considered to sharply control Type I error rate
543 when unsure of Type I error control due to pedigree structures or for small
544 numbers of variants at the expense of longer computing time. However, since
545 only small p-values are relevant, application of the bootstrap can be limited

546 to the hits obtained from the asymptotic p-value computation, mitigating the
547 computational requirements. Interestingly, the non-parametric bootstrap proce-
548 dure offers faster running times for generating 10,000 samples when considering
549 CRHs as functional annotations, ranging from the single to double, depending
550 on the type of annotations considered (Table 1).

551 Moreover, RetroFun-RVS in its current form is restricted to binary pheno-
552 types and does not allow the integration of individual-level covariates, such as
553 sex, age or genetic principal components. Hence, future work is needed to extend
554 the framework to cases selected by extreme values of continuous phenotypes and
555 to include covariates.

556 We argue that the performance of the proposed method is strongly dependen-
557 dent to the availability of the relevant tissue for the studied disease. Indeed,
558 regulatory mechanisms operate in a tissue- or cell-type-specific manner. Our
559 framework, by allowing the incorporation of several functional annotations from
560 diverse tissues or cell-types without loss of power, is useful to highlight the un-
561 derlying biological mechanisms involved in the trait. This aspect is central from
562 a fine-mapping perspective, thus RetroFun-RVS will be an important tool to
563 pinpoint causal variants located within non-coding regions, which could have
564 been missed so far.

565 8 Data and Code Availability

566 Cis-Regulatory Hubs and Topologically associated domains used in this paper
567 are available on <https://github.com/lmangnier/CRHs>. Variant data were avail-
568 able from the 1000 Genome project: [https://www.internationalgenome.org/data-
569 portal/data-collection/phase-3](https://www.internationalgenome.org/data-portal/data-collection/phase-3). The data of the Eastern Quebec SZ and BD
570 kindred study are available on request from the corresponding author. We have
571 implemented RetroFun-RVS in a R package, available on GitHub
572 (<https://github.com/lmangnier/RetroFun-RVS>). The code for the simulation
573 study is at https://github.com/lmangnier/Simulation_RL and the code for the
574 processing and analysis of the Eastern Quebec schizophrenia and bipolar disor-
575 der kindred study whole genome sequence data is at https://github.com/abureau/RV_in_SZ_BD_kindreds.

576 9 Conflict of Interest

577 The authors declare that they have no conflict of interest.

578 References

- 579 [1] Manolio, T. A., Collins, F. S., Cox, N. J., Goldstein, D. B., Hindorff, L. A.,
580 Hunter, D. J., McCarthy, M. I., Ramos, E. M., Cardon, L. R., Chakravarti,
581 A. *et al.* (2009). Finding the missing heritability of complex diseases. *Nature*
582 *461*, 747–753.

- 583 [2] Singh, T., Poterba, T., Curtis, D., Akil, H., Al Eissa, M., Barchas, J. D.,
584 Bass, N., Bigdeli, T. B., Breen, G., Bromet, E. J. *et al.* (2022). Rare coding
585 variants in ten genes confer substantial risk for schizophrenia. *Nature* *604*,
586 509–516.
- 587 [3] Sun, B. B., Kurki, M. I., Foley, C. N., Mechakra, A., Chen, C. Y., Marshall,
588 E., Wilk, J. B., Sun, B. B., Ghen, C. Y., Marshall, E. *et al.* (2022). Genetic
589 associations of protein-coding variants in human disease. *Nature* *603*, 95–
590 102.
- 591 [4] Zhang, F. and Lupski, J. R. (2015). Non-coding genetic variants in human
592 disease. *Human Molecular Genetics* *24*, R102–R110.
- 593 [5] Schaid, D. J., Chen, W., and Larson, N. B. (2018). From genome-wide as-
594 sociations to candidate causal variants by statistical fine-mapping. *Nature*
595 *Reviews Genetics* *19*, 491–504.
- 596 [6] Madsen, B. E. and Browning, S. R. (2009). A groupwise association test
597 for rare mutations using a weighted sum statistic. *PLoS Genetics* *5*.
- 598 [7] Li, B. and Leal, S. M. (2008). Methods for Detecting Associations with
599 Rare Variants for Common Diseases: Application to Analysis of Sequence
600 Data. *American Journal of Human Genetics* *83*, 311–321.
- 601 [8] Ionita-Laza, I., Buxbaum, J. D., Laird, N. M., and Lange, C. (2011). A
602 new testing strategy to identify rare variants with either risk or protective
603 effect on disease. *PLoS Genetics* *7*.
- 604 [9] Neale, B. M., Rivas, M. A., Voight, B. F., Altshuler, D., Devlin, B., Orho-
605 Melander, M., Kathiresan, S., Purcell, S. M., Roeder, K., and Daly, M. J.
606 (2011). Testing for an unusual distribution of rare variants. *PLoS Genetics*
607 *7*.
- 608 [10] Wu, M. C., Lee, S., Cai, T., Li, Y., Boehnke, M., and Lin, X. (2011). Rare-
609 variant association testing for sequencing data with the sequence kernel
610 association test. *American Journal of Human Genetics* *89*, 82–93.
- 611 [11] Laird, N. M. and Lange, C. (2006). Family-based designs in the age of
612 large-scale gene-association studies. *Nature Reviews Genetics* *7*, 385–394.
- 613 [12] Li, M., Boehnke, M., and Abecasis, G. R. (2006). Efficient study designs
614 for test of genetic association using sibship data and unrelated cases and
615 controls. *American Journal of Human Genetics* *78*, 778–792.
- 616 [13] Ott, J., Kamatani, Y., and Lathrop, M. (2011). Family-based designs for
617 genome-wide association studies. *Nature Reviews Genetics* *12*, 465–474.
- 618 [14] Bureau, A., Parker, M. M., Ruczinski, I., Taub, M. A., Marazita, M. L.,
619 Murray, J. C., Mangold, E., Noethen, M. M., Ludwig, K. U., Hetmanski,
620 J. B. *et al.* (2014). Whole Exome sequencing of distant relatives in multiplex

- 621 families implicates rare variants in candidate genes for oral clefts. *Genetics*
622 *197*, 1039–1044.
- 623 [15] Bureau, A., Begum, F., Taub, M. A., Hetmanski, J. B., Parker, M. M.,
624 Albacha-Hejazi, H., Scott, A. F., Murray, J. C., Marazita, M. L., Bailey-
625 Wilson, J. E. *et al.* (2019). Inferring disease risk genes from sequencing
626 data in multiplex pedigrees through sharing of rare variants. *Genetic Epi-*
627 *demiology 43*, 37–49.
- 628 [16] Sul, J. H., Cade, B. E., Cho, M. H., Qiao, D., Silverman, E. K., Redline,
629 S., and Sunyaev, S. (2016). Increasing Generality and Power of Rare-
630 Variant Tests by Utilizing Extended Pedigrees. *American Journal of Human*
631 *Genetics 99*, 846–859.
- 632 [17] Zhao, L., He, Z., Zhang, D., Wang, G. T., Renton, A. E., Vardarajan, B. N.,
633 Nothnagel, M., Goate, A. M., Mayeux, R., and Leal, S. M. (2019). A Rare
634 Variant Nonparametric Linkage Method for Nuclear and Extended Pedi-
635 grees with Application to Late-Onset Alzheimer Disease via WGS Data.
636 *American Journal of Human Genetics 105*, 822–835.
- 637 [18] Schaid, D. J., McDonnell, S. K., Riska, S. M., Carlson, E. E., and Thi-
638 bodeau, S. N. (2010). Estimation of genotype relative risks from pedigree
639 data by retrospective likelihoods. *Genetic Epidemiology 34*, 287–298.
- 640 [19] Li, W., Baumbach, J., Mohammadnejad, A., Brasch-Andersen, C., Vandin,
641 F., Korbel, J. O., and Tan, Q. (2019). Enriched power of disease-concordant
642 twin-case-only design in detecting interactions in genome-wide association
643 studies. *European Journal of Human Genetics 27*, 631–636.
- 644 [20] Schaid, D. J., McDonnell, S. K., Sinnwell, J. P., and Thibodeau, S. N.
645 (2013). Multiple Genetic Variant Association Testing by Collapsing and
646 Kernel Methods With Pedigree or Population Structured Data. *Genetic*
647 *Epidemiology 37*, 409–418.
- 648 [21] He, Z., Xu, B., Lee, S., and Ionita-Laza, I. (2017). Unified Sequence-Based
649 Association Tests Allowing for Multiple Functional Annotations and Meta-
650 analysis of Noncoding Variation in MetaboChip Data. *American Journal of*
651 *Human Genetics 101*, 340–352.
- 652 [22] Ma, Y. and Wei, P. (2019). FunspU: A versatile and adaptive multiple
653 functional annotation-based association test of whole-genome sequencing
654 data. *PLoS Genetics 15*, 1–21.
- 655 [23] Liu, Y., Chen, S., Li, Z., Morrison, A. C., Boerwinkle, E., and Lin, X.
656 (2019). ACAT: A Fast and Powerful p Value Combination Method for
657 Rare-Variant Analysis in Sequencing Studies. *American Journal of Human*
658 *Genetics 104*, 410–421.

- 659 [24] Fulco, C. P., Nasser, J., Jones, T. R., Munson, G., Bergman, D. T., Sub-
660 ramanian, V., Grossman, S. R., Anyoha, R., Doughty, B. R., Patwardhan,
661 T. A. *et al.* (2019). Activity-by-contact model of enhancer–promoter reg-
662 ulation from thousands of CRISPR perturbations. *Nature Genetics* *51*,
663 1664–1669.
- 664 [25] Yao, L., Liang, J., Ozer, A., Leung, A. K.-Y., Lis, J. T., and Yu, H.
665 (2022). A comparison of experimental assays and analytical methods for
666 genome-wide identification of active enhancers. *Nature Biotechnology* *40*,
667 1056–1065.
- 668 [26] Nasser, J., Bergman, D. T., Fulco, C. P., Guckelberger, P., Doughty, B. R.,
669 Patwardhan, T. A., Jones, T. R., Nguyen, T. H., Ulirsch, J. C., Lekschas,
670 F. *et al.* (2021). Genome-wide enhancer maps link risk variants to disease
671 genes. *Nature* *593*, 238–243.
- 672 [27] Gazal, S., Weissbrod, O., Hormozdiari, F., Dey, K., Nasser, J., Jagadeesh,
673 K., Weiner, D., Shi, H., Fulco, C., O’Connor, L. *et al.* (2022). Combining
674 SNP-to-gene linking strategies to pinpoint disease genes and assess disease
675 omnigenicity. *Nature Genetics* *54*, 827–836.
- 676 [28] Ma, S., Dagleish, J., Lee, J., Wang, C., Liu, L., Gill, R., Buxbaum, J. D.,
677 Chung, W. K., Aschard, H., Silverman, E. K. *et al.* (2021). Powerful gene-
678 based testing by integrating long-range chromatin interactions and knockoff
679 genotypes. *Proceedings of the National Academy of Sciences of the United*
680 *States of America* *118*, 1–12.
- 681 [29] Wu, C. and Pan, W. (2018). Integration of enhancer-promoter interac-
682 tions with GWAS summary results identifies novel schizophrenia-associated
683 genes and pathways. *Genetics* *209*, 699–709.
- 684 [30] Mangnier, L., Joly-Beauparlant, C., Droit, A., Steve, B., and Bureau, A.
685 (2022). Cis-regulatory hubs: a new 3D model of complex disease genetics
686 with an application to schizophrenia. *Life Science Alliance* *5*, 1–12.
- 687 [31] Sherman, T., Fu, J., Scharpf, R. B., Bureau, A., and Ruczinski, I. (2019).
688 Detection of rare disease variants in extended pedigrees using RVS. *Bioin-*
689 *formatics* *35*, 2509–2511.
- 690 [32] Li, B., Wang, G. T., and Leal, S. M. (2015). Generation of sequence-based
691 data for pedigree-segregating Mendelian or Complex traits. *Bioinformatics*
692 *31*, 3706–3708.
- 693 [33] Maziade, M., Roy, M.-A., Chagnon, Y. C., Cliche, D., Fournier, J.-P.,
694 Montgrain, N., Dion, C., Lavallée, J.-C., Garneau, Y., Gingras, N. *et al.*
695 (2005). Shared and specific susceptibility loci for schizophrenia and bipolar
696 disorder: a dense genome scan in eastern quebec families. *Mol Psychiatry*
697 *10*, 486–99.

- 698 [34] Awadalla, P., Boileau, C., Payette, Y., Idaghmour, Y., Goulet, J.-P., Knop-
699 pers, B., Hamet, P., Laberge, C., and CARTaGENE Project (2013). Cohort
700 profile of the cartagene study: Quebec's population-based biobank for pub-
701 lic health and personalized genomics. *Int J Epidemiol* *42*, 1285–99.

CRHs	RetroFun-RVS		Sliding	RV-NPL	CHP-NPL	RVS	
	G-E Pairs	Genes		All + Pairs	All + Pairs	Complete	Partial
1.06 (1665.06)	2.02 (3363.39)	1.11 (2979.89)	11.05 (3603.92)	971.4	1823.4	14.26	443.5

Table 1: Running times (in seconds) for analyzing rare variants in the TAD, in one simulated replicate, using a single 2.10GHz processor. For RetroFun-RVS, we also provided average running times for computing empirical p-values based on 10,000 samples (in parenthesis). For RV-NPL empirical p-values were obtained based on 1 million permutations.

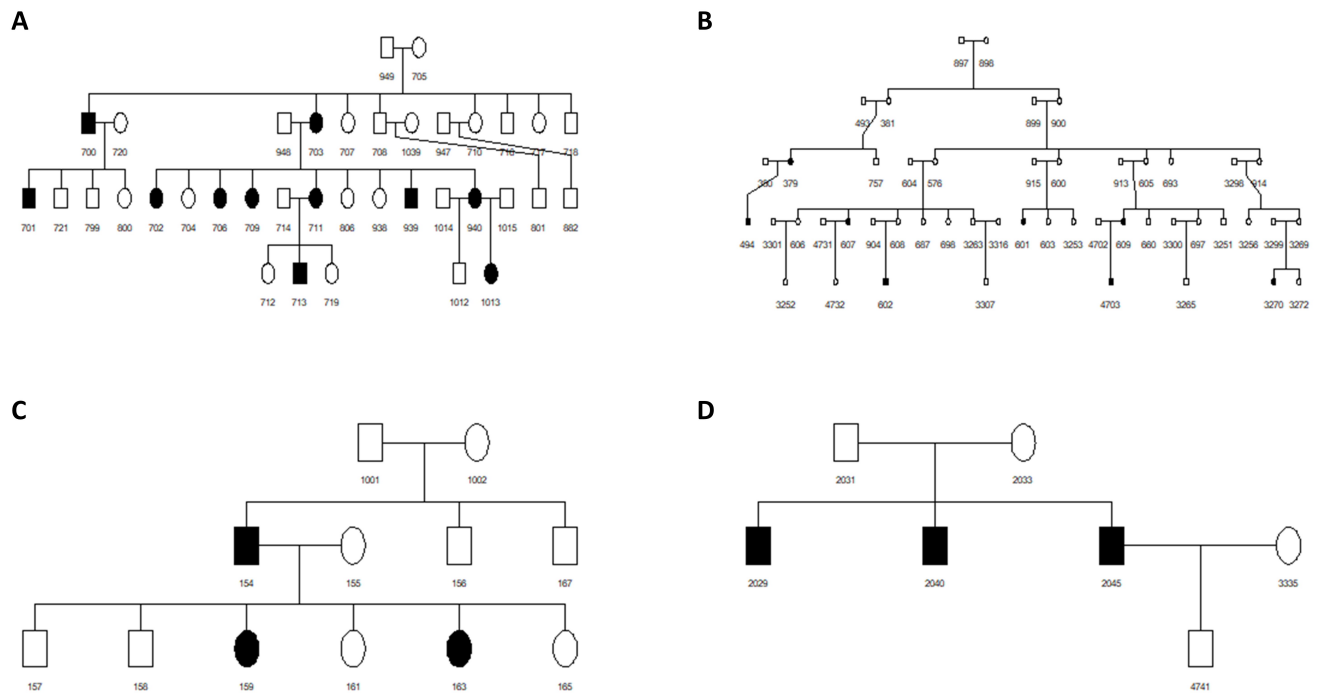


Figure 1: Example of pedigree structures considered in the simulation studies. Affected subjects are indicated by filled squares or circles

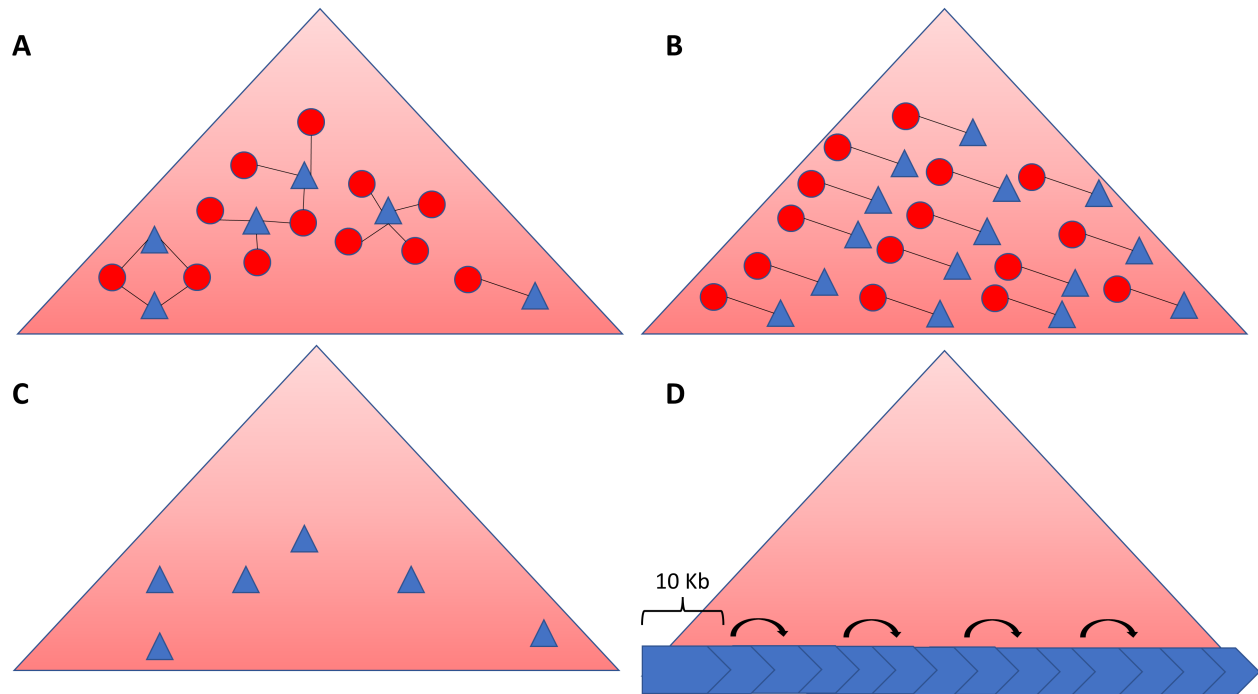


Figure 2: Overview of functional annotations considered in the simulation studies. For all 4 panels, big red triangles represent the selected TAD for the simulation studies, small blue triangles the genes (exons + promoters), and red circles the enhancers. (A) CRHs as functional annotations. (B) Pairs as functional annotations. CRHs are split with respect to each gene-enhancer pair. (C) Genes as functional annotations. (D) 10 Kb sliding windows as functional annotations.

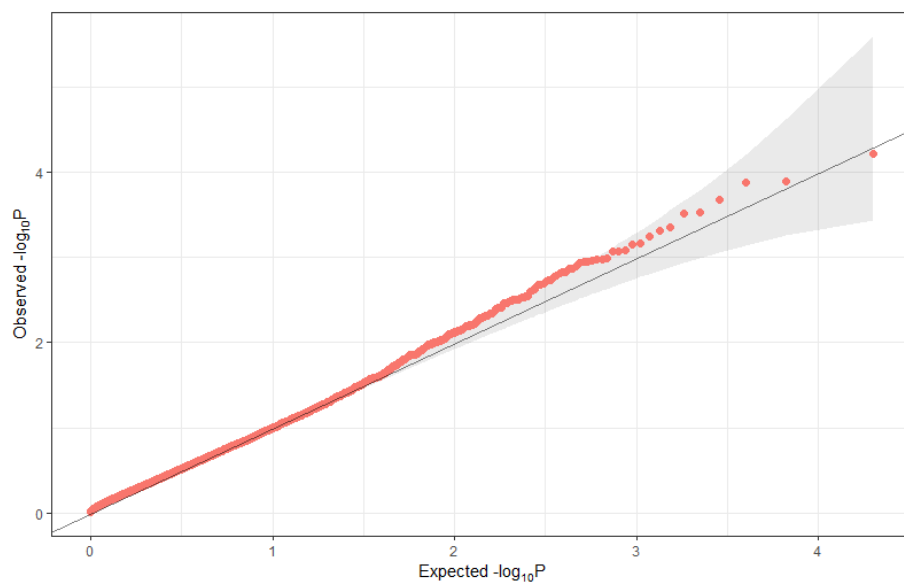


Figure 3: Quantile-Quantile plot of ACAT-Combined P-values for RetroFun-RVSCRHs considering variant dependence. We omitted CRHs with a number of families less than 5 ensuring a proper asymptotic behavior.

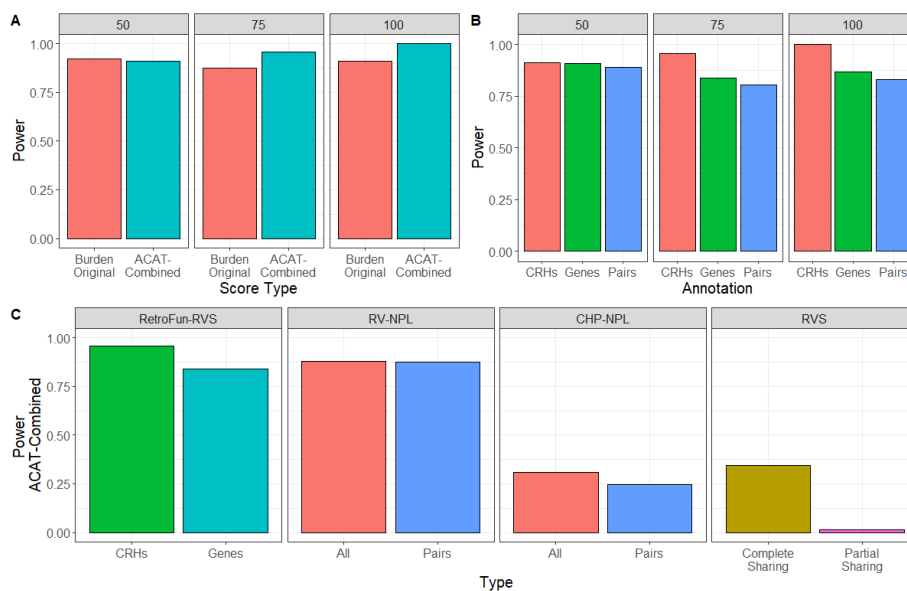


Figure 4: Power evaluation of RetroFun-RVS under different scenarios for 2% risk variants. (A) Power at different proportions of risk variants within the CRH, between $\text{RetroFun-RVS}_{CRHs}$ with no functional annotation (Burden Original) and $\text{RetroFun-RVS}_{CRHs}$ including the four CRHs (ACAT-Combined). Power was evaluated on 1,000 replicates. (B) Power at different proportions of risk variants within the CRH between $\text{RetroFun-RVS}_{CRHs}$ (CRHs), $\text{RetroFun-RVS}_{Pairs}$ (G-E Pairs), $\text{RetroFun-RVS}_{Genes}$ (Genes), and $\text{RetroFun-RVS}_{Sliding-Window}$ (Sliding). Functional annotations with fewer than five families were removed from the analysis for ensuring a proper asymptotic behavior. Given the Type I error inflation observed for $\text{RetroFun-RVS}_{Sliding-Window}$, this approach was excluded from the power comparison. Power was evaluated on 1,000 replicates. (C) Power at 75% risk variants within one CRH between $\text{RetroFun-RVS}_{CRHs}$ and other affected-only competing methods. Here we included $\text{RetroFun-RV}_{genes}$ to mimic CHP-NPL procedure. Power for $\text{RetroFun-RVS}_{CRHs}$ and $\text{RetroFun-RVS}_{Genes}$ was evaluated on 1,000 replicates, while for RV-NPL and RVS we generated 200 replicates.